

First Order Phase Transitions in Neutron Star Matter: Droplets and Coherent Neutrino Scattering

Sanjay Reddy¹, George Bertsch¹ and Madappa Prakash²

¹*Institute For Nuclear Theory, University of Washington, Seattle, WA 98195.*

²*Dept. Physics & Astronomy, SUNY at Stony Brook, Stony Brook, NY 11794.*

(August 12, 2018)

A first order phase transition at high baryon density implies that a mixed phase can occupy a significant region of the interior of a neutron star. In this article we investigate the effect of a droplet phase on neutrino transport inside the core. Two specific scenarios of the phase transition are examined, one having a kaon condensate and the other having quark matter in the high density phase. The coherent scattering of neutrinos off the droplets greatly increases the neutrino opacity of the mixed phase. We comment on how the existence of such a phase will affect a supernova neutrino signal.

PACS numbers(s): 13.15.+g, 26.60.+c, 97.60.Jd

Neutrino interactions play a central role in the early evolution of neutron stars formed during a type II supernova. The enormous binding energy ($\sim 10^{53}$ ergs) gained during implosion of the inner core of a massive star is released in the form of neutrinos. Temporal and spectral characteristics of the neutrino emission from the newly born neutron star, also called a protoneutron star, influences the explosion mechanism, the r-process nucleosynthesis, and more importantly, is an observable feature of a supernova explosion. The handful of neutrino events observed from SN87A are testimony to this fact.

In this article we study how a first order phase transition at high density will influence the neutrino opacity. We consider two models of high density matter wherein a first order phase transition occurs for densities of relevance for neutron stars: first order kaon condensation and the quark-hadron transition. The mixed phase consists of a high baryon density, negatively charged, kaon condensed matter or quark matter coexisting with lower density, positively charged, baryonic matter. We study the region of the mixed phase where the structure is expected to be droplets of kaonic matter or quark matter embedded in a lower baryon density nucleonic matter. Our primary motivation for this study is to determine the neutrino opacity of this material since this is directly related to an observable - the supernova neutrino luminosity curve.

Our main finding is that the neutrino mean free path in a mixed phase containing either kaon condensed matter or quark matter is greatly reduced compared to uniform baryonic matter at the same density. This is a consequence of the coherent scattering of neutrinos from the matter in the droplets. The droplets carry a large weak charge and scattering of long-wavelength neutrinos increases as its square. The reduction of the mean free path compared to that in pure neutron matter could be as large as one to two orders of magnitude. Thus, despite our poor knowledge of neutrino opacities in dense nucleonic matter, we argue that the presence of a first order phase transition is likely to have a dramatic and discernible effect on the temporal characteristics of supernova neutrino light curve.

Neutrino-Droplet Scattering: Prior to discussing in detail the specific models in which a droplet phase is energetically favored, we describe neutrino-droplet scattering. Neutrinos scatter off the droplets as they carry a net excess of weak-charge. For the typical droplet sizes which range from 5 – 15 fm we may infer that the scattering will be fairly coherent for momentum transfers $\lesssim 40$ MeV.

First, we consider neutrino scattering from isolated droplets. The Lagrangian that describes the neutral current coupling of neutrinos to the droplet is given by

$$\mathcal{L}_W = \frac{G_F}{2\sqrt{2}} \bar{\nu} \gamma_\mu (1 - \gamma_5) \nu J_D^\mu. \quad (1)$$

where J_D^μ is the neutral current carried by the droplet and $G_F = 1.166 \times 10^{-5}$ GeV⁻² is the Fermi weak coupling constant. For non-relativistic droplets $J_D^\mu = \rho_W(x) \delta^{\mu 0}$ has only a time like component and $\rho_W(x)$ is the excess weak charge density in the droplet. The total weak charge enclosed in a droplet of radius r_d is given by $N_W = \int_0^{r_d} d^3x \rho_W(x)$ and the form factor is $F(q) = (1/N_W) \int_0^{r_d} d^3x \rho_W(x) \sin qx/qx$. The differential cross section for neutrinos scattering from an isolated droplet is then given by

$$\frac{d\sigma}{d \cos \theta} = \frac{E_\nu^2}{16\pi} G_F^2 N_W^2 (1 + \cos \theta) F^2(q). \quad (2)$$

In the above equation E_ν is the neutrino energy and θ is the scattering angle. Since the droplets are massive we consider only elastic scattering in which case the magnitude of the momentum transfer is given by $q = \sqrt{2} E_\nu (1 - \cos \theta)$.

Neutrino transport in the mixed phase: We must also embed the droplets into a description of the medium to evaluate the neutrino transport parameters. The droplet radius r_d and the inter-droplet spacing are determined by the interplay of surface and Coulomb energies and depends on the specific details of the high density model. We will calculate the droplets in the Wigner-Seitz cell assuming that the medium has a droplet density N_D . The cell radius $R_W = (3/4\pi N_D)^{1/3}$. Except for one aspect, we will neglect the coherent scattering from more than one droplet. If the droplets form a lattice, Bragg scattering will dominate and our description would not be valid. But for a low density and a liquid phase the interference from multiple droplets affects only the scattering at long wavelengths. If the ambient temperature is not small compared to the melting temperature the droplet phase will be a liquid and for neutrino energy in the range $E_\nu \gtrsim (1/R_W)$ interference effects arising from scattering off different droplets is small. However, multiple droplet scattering cannot be neglected for $E_\nu \lesssim 1/R_W$. The effects of other droplets is to cancel the scattering in the forward direction, because the interference is destructive except at exactly zero degrees, where it produces a change in the index of refraction of the medium. We account for this by subtracting from the weak charge density ρ_W a uniform density which has the same total weak charge N_W as the matter in the Wigner-Seitz cell. The effect on the form factor is to modify it as follows

$$F(q) \rightarrow \tilde{F}(q) = F(q) - 3 \frac{\sin qR_W - (qR_W) \cos qR_W}{(qR_W)^3}. \quad (3)$$

In the medium, the appropriate differential cross section is defined per unit volume rather than per droplet. The neutrino-droplet differential cross section per unit volume follows from the preceding discussion and is given by

$$\frac{1}{V} \frac{d\sigma}{d\cos\theta} = N_D \frac{E_\nu^2}{16\pi} G_F^2 N_W^2 (1 + \cos\theta) \tilde{F}^2(q). \quad (4)$$

Note that even for small droplet density N_D the factor N_W^2 acts to enhance the droplet scattering. To quantify the importance of droplets as a source of opacity we compare with the standard scenario where matter is uniform and composed of neutrons. In this case the dominant source of opacity is due to scattering from thermal fluctuations and the cross section per unit volume is given by

$$\begin{aligned} \frac{d\sigma}{V d\cos\theta} &= \frac{G_F^2}{8\pi} (c_V^2 (1 + \cos\theta) + (3 - \cos\theta) c_A^2) E_\nu^2 \\ &\times \frac{3}{2} n_n \left[\frac{k_B T}{E_{fn}} \right], \end{aligned} \quad (5)$$

where c_V, c_A are the vector and axial coupling constants of the neutron, n_n is neutron number density, E_{fn} is the neutron Fermi energy and T is the matter temperature [1,2].

The transport cross sections that are employed in studying the diffusive transport of neutrinos in the core are weighted by the angular factor $(1 - \cos\theta)$. The transport mean free path $\lambda(E_\nu)$ for given neutrino energy E_ν is given by

$$\frac{1}{\lambda(E_\nu)} = \frac{\sigma_T(E_\nu)}{V} = \int d\cos\theta (1 - \cos\theta) \left[\frac{1}{V} \frac{d\sigma}{d\cos\theta} \right]. \quad (6)$$

It is thus the task of the models to provide the weak charge and form factors of the droplets so that we may calculate the contribution of neutrino-droplet scattering to the opacity of the mixed phase.

First-order Kaon condensation Kaon condensation is one of the several possible forms of exotica that could exist at high baryon density. Since the pioneering work of Kaplan and Nelson [3] several authors (see [4,5] and references therein) have studied in detail the role of such a condensate in neutron star structure and evolution. Kaon condensation significantly softens the high density equation of state (EOS) thereby lowering the maximum mass of neutron stars. Glendenning and Schaffner [6] revisited the problem and studied kaon condensation in a relativistic mean field model, wherein the kaon is minimally coupled to σ , ω and ρ mesons. Within the purview of this model they were able to show that kaon condensation occurs as a first order phase transition.

A relativistic field theoretical approach is used to describe the baryons. We follow the model employed by Glendenning and Schaffner [6] wherein the Lagrangian density is given by

$$\begin{aligned} L &= \sum_B \bar{B} (i\gamma^\mu \partial_\mu - g_{\omega B} \gamma^0 \omega_0 - g_{\rho B} \gamma^0 \mathbf{b}_0 \cdot \mathbf{t} \\ &- M_B + g_{\sigma B} \sigma) B \\ &+ \frac{1}{2} m_\omega^2 \omega_0^2 + \frac{1}{2} m_\rho^2 b_0^2 - \frac{1}{2} m_\sigma^2 \sigma^2 - U(\sigma). \end{aligned}$$

Here, B are the Dirac field operators for baryons and \mathbf{t} is the isospin matrix. In the mean field approximation only the zeroth components of the sigma, omega and rho meson fields are retained and are denoted by σ, ω_0 and b_0 respectively. $U(\sigma)$ represents the scalar self-interactions and is of the form $U(\sigma) = (b/3)M_n(g_{\sigma N}\sigma)^3 + (c/4)(g_{\sigma N}\sigma)^4$. Kaons are coupled minimally to the meson fields appearing in the baryonic part of the Lagrangian. The Lagrange density for the kaon field is given by

$$L_K = \mathcal{D}_\mu^* K^* \mathcal{D}^\mu K - (m_K - g_{\sigma K}\sigma)^2 K^* K,$$

where the covariant derivative

$$\mathcal{D}_\mu = (\partial_\mu + i(g_{\omega K}\omega_\mu + g_{\rho K}b_\mu)).$$

Droplets are constructed in the Thomas-Fermi or local density approximation. The equation of motion for the kaons is given by

$$[\mathcal{D}_\mu \mathcal{D}^\mu + (m_K^*)^2] K^- = 0, \quad (7)$$

where $m_K^* = m_K - g_{\sigma K}\sigma$ is the kaon effective mass in the medium. Eq. (7) is solved by writing explicitly the spatial and temporal dependence of the kaon field as $K^- = f_\pi \theta(r) \exp(i\mu_K t) / \sqrt{2}$ where $f_\pi = 93$ MeV is the pion decay constant. The spatial part has only a radial dependence, and the time dependence is fixed by the chemical potential [7]. In principle we should solve a Klein-Gordon equation for the other meson fields as well. However, the other mesons are significantly more massive and their fields do not vary over distances of the order of their Compton wavelengths. In the vicinity of the critical density the effective kaon mass is approximately given by $m_K^* \sim \mu_e \sim 200$ MeV and is small compared to σ, ω or ρ meson masses. In this approximation the non-strange meson field equations are

$$m_\sigma^2 \sigma = -\frac{dU}{d\sigma} + g_{\sigma B}(\rho_n^s + \rho_p^s) + g_{\sigma k} f_\pi^2 \theta^2 m_k^*, \quad (8)$$

$$m_\omega^2 \omega_0 = g_\omega(\rho_n + \rho_p) - g_{\omega K}^2 f_\pi^2 \theta^2 (\mu_K + X), \quad (9)$$

$$m_\rho b_0 = \frac{1}{2} g_\rho (\rho_p - \rho_n) - g_{\rho K} f_\pi^2 \theta^2 (\mu_K + X). \quad (10)$$

where ρ_n, ρ_p, ρ_n^s and ρ_p^s are the baryon number and scalar densities of the neutrons and protons respectively and the vector potential for the kaons is given by $X = g_{\omega k}\omega_0 + g_{\rho k}b_0$.

The classical kaon field equation is obtained by substituting the specific form given above in Eq.(7) and is given by

$$-\nabla^2 \theta(r) + [(\mu_K + X)^2 - (m_k - g_{\sigma K}\sigma)^2] \theta(r) = 0. \quad (11)$$

The above differential equation is solved with appropriate boundary conditions to obtain the droplet configuration. The baryon and electron chemical potentials are close to those in the mixed phase, but must be fine tuned to give a solution to Eq.(11) that satisfies the boundary conditions at both $r = 0$ and $r = R_W$. The energy is computed in the Wigner-Seitz approximation and the droplet radius that minimizes the energy density is determined. The energy density contains bulk, surface and Coulomb contributions. The baryonic contribution is

$$\epsilon_B(r) = \epsilon_{kin} + \frac{1}{2} m_\sigma^2 \sigma^2 + \frac{1}{2} m_\omega^2 \omega_0^2 + \frac{1}{2} m_\rho^2 b_0^2 + U(\sigma_o), \quad (12)$$

and the kaon contribution is given by

$$\epsilon_k(r) = f_\pi^2 \theta^2(r) (\mu_K + X)^2. \quad (13)$$

Note that the surface contribution is contained in the above expression and that terms proportional to the gradients have been eliminated by using the equation of motion for the kaons.

The shape of the cell depends on the type of lattice that is favored; for BCC or FCC the Wigner-Seitz cell is a regular polyhedron and can be approximated by a sphere. The Wigner-Seitz radius, denoted by R_W , is determined by size of the cell that encloses zero total electric charge. Since the electric field vanished at $r = R_W$, the Coulomb energy is given by

$$E_c = \frac{\alpha}{2} \int_0^{R_W} dr \frac{Q_e^2(r)}{r^2}, \quad (14)$$

where $\alpha = 1/137$ and $Q_e(r)$ is the enclosed electric charge a distance r from the center.

We find that the Debye screening lengths $(1/\lambda_D^2)_i = 4\pi\alpha(\partial n_i/\partial\mu_i)_{n_j, j\neq i}$ of electrons, protons and kaons are of the same order as that the typical droplet radius. Thus the charged particle distributions may change and screen the droplet charge [8]. We allow for this by adding the Coulomb term to the single particle energies and employing a iterative procedure to relax the charged particle distributions to their equilibrium value. For droplets radii $r_d \sim \lambda_D$ the charge particle distributions in the droplet changes at the 10-30 percent level depending on their individual Debye screening lengths. However, for $r_d/\lambda_D \gg 1$ the charge particle distributions change drastically and all the charge resides in the surface region. For these conditions the droplet phase is not energetically favored [8]. Our investigation indicates that for baryon density in the region $0.52 - 0.62 \text{ fm}^{-3}$ the droplets survive, but with moderate modifications to the charged particle profiles. Fig. 1 shows the particle density profiles at $n_B = 0.54 \text{ fm}^{-3}$.

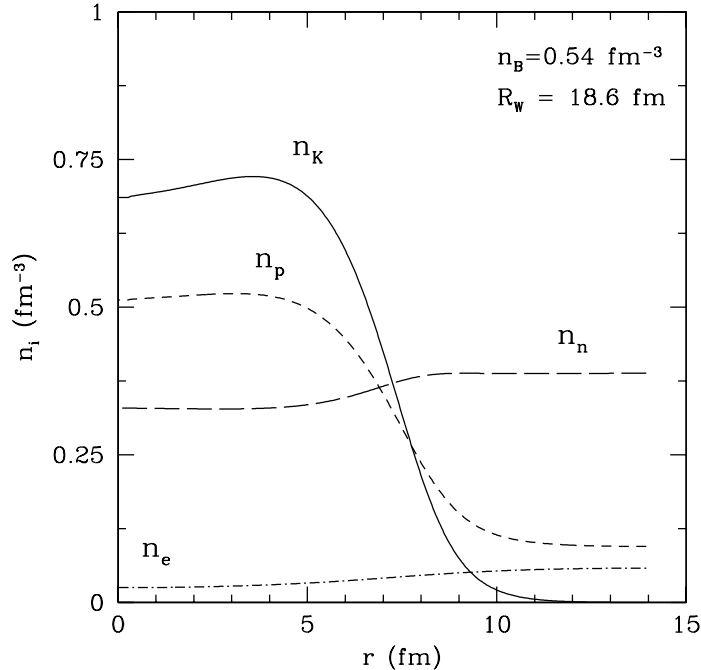


FIG. 1. Droplet profile at baryon density $n_B = 0.54 \text{ fm}^{-3}$. The solid curve shows the kaon number density, the short-dashed and long-dashed curves show the proton and neutron number densities respectively. The kaon, proton, neutron and electron number densities are shown as solid, dashed, long-dashed and dot-dashed curves respectively.

The excess vector weak charge density of the droplet is

$$\begin{aligned} \rho_W(r) = & (-1 + 2 \sin^2 \theta_W) n_K(r) \\ & + (1 + 4 \sin^2 \theta_W) (n_e(r) - n_e^o) \\ & + (1 - 4 \sin^2 \theta_W) (n_p(r) - n_p^o) - (n_n(r) - n_n^o), \end{aligned} \quad (15)$$

where n_K, n_e, n_p and n_n are the kaon, electron, proton and neutron number densities respectively and n_e^o, n_p^o and n_n^o are corresponding densities in the low density phase. Kaons dominate the weak charge density since (i) the electron number is small, (ii) the protons carry negligible weak charge, and (iii) the neutron number density inside and outside the droplet are nearly equal. The neutral current neutrino-kaon coupling is not experimentally measured and our estimates here are based on the constituent quark model (note that the main source of uncertainty is the singlet contribution [9], in the large N_C limit that the singlet current contributes at the 30 percent level to the weak charge of the kaon). The total weak charge of the droplet shown in Fig. 1 is $N_W \simeq 700$. The corresponding form factor $F(q)$ is shown in the top panel of Fig. 2.

The transport differential scattering (Eq.(2)) weighted with the factor $(1 - \cos\theta)$ for $E_\nu = 50 \text{ MeV}$ and for a baryon density of $n_B = 0.54 \text{ fm}^{-3}$ is shown in the bottom panel of Fig. 2. For comparison we also show results for uniform neutron matter (computed by using Eq.(5) and for $T = 10 \text{ MeV}$) where thermal density fluctuations dominate the opacity.

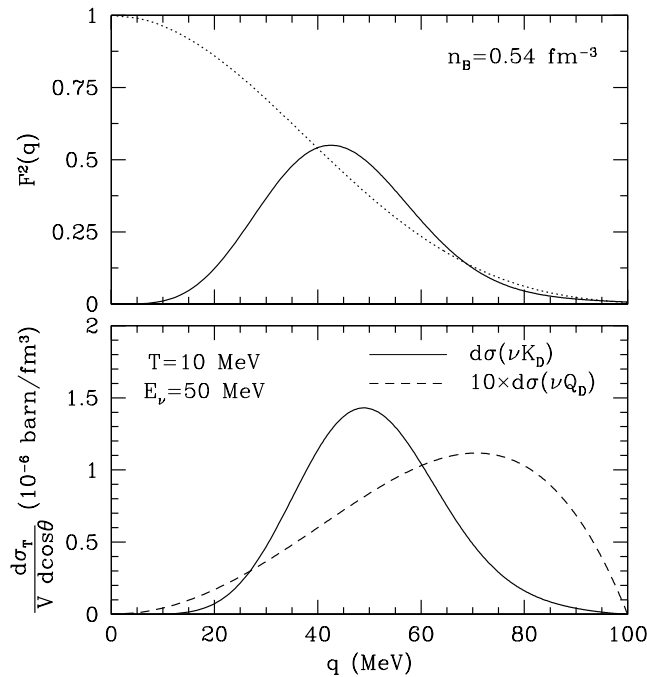


FIG. 2. Top panel: The dashed curve shows the form factor for a single drop and the solid curve shows the results for an embedded droplet (Eq.(3)). Lower panel: Transport differential cross section for scattering off droplets (solid curve) and for scattering off thermal fluctuations in pure neutron matter (dashed curve). Note that dashed curve has been multiplied by a factor of 10.

The neutrino mean free path computed using Eq.(4) is shown (solid curve) in Fig. 3 for $n_B = 0.54$ and for a temperature of 10 MeV. The mean free path in uniform neutron matter is also shown (dashed curve) for comparison. As is evident from the figure, the mean free path in the mixed phase is significantly reduced compared to pure neutron matter for typical neutrino energy $E_\nu \sim \pi T$. The reduction is severe at moderate energies, and is easily understood by noting that the form factors have significant support in the region where $q \sim 40$ MeV. At lower q the inter-droplet correlations act to screen the weak charge of the droplet and at higher energy is attenuated by the form factor. Although the transport calculations would require the energy dependent mean free path it is useful to define an average mean free path for energy transport $\langle \lambda_E \rangle = \int dE_\nu f_\nu(E_\nu) E_\nu^4 \lambda(E_\nu) / (\int dE_\nu f_\nu(E_\nu) E_\nu^4)$ where $f_\nu(E_\nu)$ is the neutrino distribution function [2]. At $T = 10$ MeV we find that $\langle \lambda_E \rangle$ is reduced by a factor ~ 20 and at $T = 30$ MeV the reduction is reduced by a factor ~ 9 .

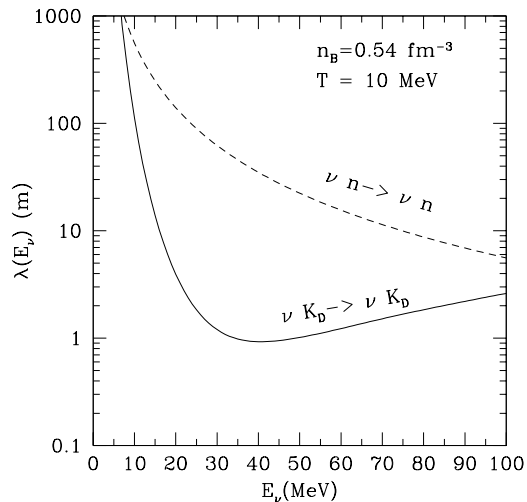


FIG. 3. Neutrino mean free path in the droplet phase. Results for neutrino droplet scattering (solid curve) are compared with the uniform neutron matter case (dashed curve).

First order quark-hadron transition Several authors have studied the possibility of a first order quark-hadron phase transition in a bag model picture for densities of relevance to neutron star interiors [11–13]. These studies found that a mixed phase was energetically favored. Detailed investigations of the structured phase by Heiselberg *et al.*, wherein surface and Coulomb contributions to the energy density were properly accounted for, showed that the presence of a droplet phase was sensitive to the value of the surface tension σ between the quark and hadron phases [8]. For $\sigma \leq 100$ MeV the droplet sizes favored were smaller than the typical Debye screening length $\lambda_D \sim 7$ fm and the droplet phase was energetically favored.

The droplet radius is given by $r_d = [15\sigma/(8\pi(\rho_Q - \rho_N)^2)]^{1/3}$, where ρ_Q and ρ_N are the electric charge densities in the quark and nucleon phases respectively. The charge densities depend in general on details of the model and a typical scale for the difference $\rho_Q - \rho_N \sim 0.4 e \text{ fm}^{-3}$. For σ in the range 10–100 MeV this corresponds to droplet radii of $r_d = 3-7$ fm. For our estimate of coherent scattering we will assume a droplet radius $r_d = 5$ fm at a baryon density $n_B = 0.7 \text{ fm}^{-3}$. In a minimal model the nucleonic phase is described by a relativistic mean field theory and the quark phase as a free Fermi gas with a bag constant [13] $B = 200 \text{ MeV/fm}^3$ and a finite strange quark mass $m_s = 150 \text{ MeV}$. In this model, and for $n_B = 0.7 \text{ fm}^{-3}$, the baryon density in the nucleon phase is $n_N = 0.68 \text{ fm}^{-3}$ and $n_Q = 0.94 \text{ fm}^{-3}$ in the quark phase. The volume fraction occupied by the quark phase is given by $f = (n_B - n_N)/(n_Q - n_N) \sim 0.1$ and the Wigner-Seitz cell radius spacing $R_W = r_d/f^{1/3} \sim 11$ fm.

For small droplets the quark densities are uniform to good approximation and are determined by conditions of local chemical equilibrium. The electron density is the same inside and outside the droplet. Thus the excess weak charge density in the quark droplet is given by

$$\begin{aligned} \rho_W = & [(n_u - (n_d + n_s)) - (n_n - n_p)] \\ & - \frac{4}{3}[n_u - (n_d + n_s) + 3n_p] \sin^2 \theta_W, \end{aligned} \quad (16)$$

where n_u, n_d, n_s are the up, down and strange quark number densities inside the droplet, and n_n, n_p the neutron and proton densities outside. The individual particle densities are shown in the Fig. 4. The net weak charge and form factor for a droplet of radius $r_d = 5$ fm and cell radius $R_W = 11$ fm are computed as described earlier. We find that the total weak charge $N_W \simeq 860$ and the droplet density $N_D = 18 \times 10^{-5} \text{ fm}^{-3}$. The transport differential cross section (left panel) and the neutrino mean free path (right panel) are shown in Fig. 5. We see that the results are qualitatively similar to those in the K^- condensate scenario. The energy averaged neutrino mean free path $\langle \lambda_E \rangle$ defined earlier at $T = 10$ MeV is reduced by a factor of ~ 10 compared to pure neutron matter and at $T = 30$ MeV is reduced by a factor ~ 17 .

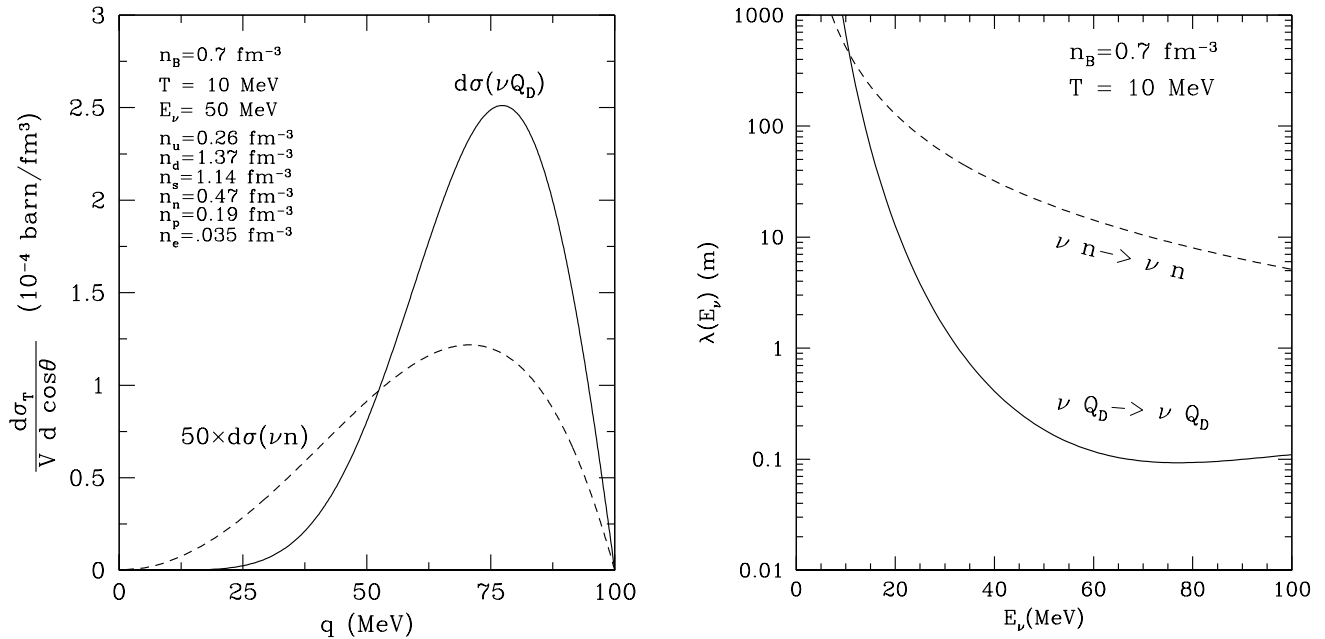


FIG. 4. Results for neutrino-quark droplet scattering (solid curve) are compared with the uniform neutron matter case (dashed curve). Left panel shows the results for the differential scattering of neutrinos with energy $E_\nu = 50$ MeV and the right panel shows the neutrino mean free path at $n_B = 0.7 \text{ fm}^{-3}$ and $T = 10$ MeV. The left panel also shows the individual particle densities in the mixed phase.

Discussion: There are several caveats to the study presented in this work which we would like to address in this paragraph. First, formula for the scattering in Eq.(3) treats the effects of droplet-droplet correlations rather crudely, and short range order between droplets could affect the low momentum transfer scattering. However, these momenta have small weight at temperatures of interest, and corrections to the transport would be small. Our treatment of the form factor at small q may be viewed as being conservative. Second, in the mixed phase we studied only droplets and ignored the possibility of other spatial structures which might exist for some range of density. Qualitatively, the heterogeneity of the mixed phase is the key feature that results in an enhanced neutrino opacity. Thus, our results provide a rough estimate of what one may expect even when the structures are more complex. Both these issues clearly require more attention and we hope to pursue this in detail in future work. Thirdly, the droplets are likely to have low lying collective modes which the neutrinos could excite. This will also make an important contribution to the opacity of the material and requires further work. Lastly, we expect that droplet formation will be fairly rapid due to the large temperatures ($T \sim 50$ MeV) reached during the implosion of the inner core.

Our main focus was to study the consequences of a first order phase transition on the transport of neutrinos in the inner core of neutron stars. We have shown that the droplet phase is indeed very opaque to neutrinos. Studies of the early evolution of neutron stars, where diffusive transport of neutrinos directly affects the temporal evolution of neutrino emission, which incorporate the effects arising due to a first order phase transition remain largely unexplored. In view of our findings in this article we may expect significant changes to the neutrino emission if a droplet phase were to exist in the inner core of a newly born neutron star. It seems likely that detailed studies of the diffusive transport of neutrinos in models with a droplet phase will provide the link between the observable features of a supernova neutrino signal and the phases of matter at high density.

The authors would like to thank Paulo Bedaque, Chuck Horowitz, David Kaplan, Thomas Papenbrock, Martin Savage and Ray Sawyer for useful discussions. We would also like to thank Jason Cooke for providing us numerical tables of his work on quark-hadron phase transitions. This work is supported by the grant DOE-FG-06-90ER40561.

- [1] R. F. Sawyer, Phys. Rev. **D11**, 2740 (1975).
- [2] S. Reddy, M. Prakash, and J. M. Lattimer, Phys. Rev. **D58**, 013009 (1998).
- [3] D. B. Kaplan and A. E. Nelson, Phys. Lett. **B 175**, 57 (1986), *ibid* B 179, 409 (E).
- [4] M. Prakash, I. Bombaci, Manju Prakash, P. J. Ellis, J. M. Lattimer, and R. Knorren, Phys. Rep **280**, 1 (1997).
- [5] H. Fujii, T. Maruyama, T. Muto, and T. Tatsumi, Nucl. Phys. **A597**, 645 (1996).
- [6] N. K. Glendenning and J. Schaffner-Bielich, Phys. Rev. Lett. **81**, 4564 (1998).
N. K. Glendenning and J. Schaffner-Bielich, Phys. Rev. C **60**, 025803, (1999).
- [7] G. Baym, Phys. Rev. Lett. **30**, 1340 (1973).
- [8] H. Heiselberg, C. J. Pethick and E. F. Staubo, Phys. Rev. Lett. **70** 1355 (1993).
- [9] Ming-Lu and M. B. Wise, Phys. Lett. **B324**, 461 (1994).
- [10] D. G. Ravenhall, C. J. Pethick and J. R. Wilson, Phys. Rev. Lett. **50** 2066 (1983).
- [11] J. C. Collins and M. J. Perry Phys. Rev.Lett **34**, 1353 (1975).
- [12] N. K. Glendenning Phys. Rev. **D46**, 1274 (1992).
- [13] M. Prakash, J. R. Cooke and J. M. Lattimer Phys. Rev. **D52**, 661 (1995).